Soil hydraulic properties in one-dimensional layered soil profile using layer-specific soil moisture assimilation scheme

Yongchul Shin,[1] Binayak P. Mohanty,[1] and Amor V. M. Ines[1,2]

Received 24 May 2010; revised 25 April 2012; accepted 14 May 2012; published 23 June 2012.

[1] We developed a layer-specific soil-moisture assimilation scheme using a simulation-optimization framework, Soil-Water-Atmosphere-Plant model with genetic algorithm (SWAP-GA). Here, we explored the quantification of the soil hydraulic properties in a layered soil column under various combinations of soil types, vegetation covers, bottom boundary conditions and soil layering using idealized (synthetic) numerical studies and actual field experiments. We demonstrated that soil layers and vertical heterogeneity (layering arrangements) could impact to the uncertainty of quantifying soil hydraulic parameters. We also found that, under layered soil system, when the subsurface flows are dominated by upward fluxes, e.g., from a shallow water table, the solution to the inverse problem appears to be more elusive. However, when the soil profile is predominantly draining, the soil hydraulic parameters could be fairly estimated well across soil layers, corroborating the results of past studies on homogenous soil columns. In the field experiments, the layer-specific assimilation scheme successfully matched soil moisture estimates with observations at the individual soil layers suggesting that this approach could be applied in real world conditions.

Citation: Shin, Y., B. P. Mohanty, and A. V. M. Ines (2012), Soil hydraulic properties in one-dimensional layered soil profile using layer-specific soil moisture assimilation scheme, *Water Resour. Res.*, *48*, W06529, doi:10.1029/2010WR009581.

1. Introduction

[2] Soil hydraulic parameters are significant components for many hydrological, meteorological, and general circulation models [*Hansen et al.*, 1999; *Mohanty et al.*, 2002; *Mohanty and Zhu*, 2007]. They are used to define the soil hydraulic properties in the vadose zone, characterizing the effective hydraulic behavior of the soil system [*Wood*, 1994; *Vrugt et al.*, 2004].

[3] With the objective of exploring the utility of remote sensing of soil moisture for deriving soil hydraulic properties at aggregate scale, *Ines and Mohanty* [2008a, 2008b, 2009] tested the hypothesis that near-surface soil moisture assimilation scheme can be used to quantify effective soil hydraulic properties of an "effective" soil column based on the inverse modeling. The effective soil column is a 'homogenous' conceptual representation of a real-world soil column (composed of soil horizons) characterized by effective soil hydraulic properties. The inverse method using near-surface soil moisture assumes that any perturbations made at the near-surface soil layer could influence the soil moisture dynamics at the subsurface and hence can inform the estimations of subsurface soil hydraulic properties. The effective soil hydraulic properties serve as "average" properties of the system. *Ines and Mohanty* [2008b] however found that if the system is highly heterogeneous, the assumption of effective soil column could fail.

[4] Understanding of how soil vertical layering might affect soil moisture exchange and soil hydraulic parameter estimations is therefore important. Significant efforts have been made to account for the impact of soil heterogeneity on field soil moisture contents. The soil hydraulic conductivity, moisture content, and soil hydraulic parameters are variable at the field scale [*Nielsen et al.*, 1973; *Stockton and Warrick*, 1971; *Jana and Mohanty*, 2012a, 2012b]. *Bosch* [1991] studied an analytical expression for forecasting (potential) errors by using point observation of the matric potential (h) to determine the average matric potential (h) in a heterogeneous column. The instantaneous profile method suggested by *Green et al.* [1986] can be used to measure hydraulic conductivities ($K(h)$) at field-scales [*Rose et al.*, 1965; *van Bavel et al.*, 1968; *Nielsen et al.*, 1973]. This method involves measurement of moisture content (θ) and matric potential (h) throughout the profile.

[5] *Zhu and Mohanty* [2002] reported various hydraulic parameter averaging schemes and the mean hydraulic conductivity for predicting the mean fluxes in the horizontal heterogeneous blocks under steady state of infiltration and evaporation using Gardner-Russo exponential model [*Gardner*, 1958] and the Brooks-Corey model [*Brooks and Corey*, 1964]. The effective hydraulic parameter estimations were related to areal soil heterogeneity and land surface conditions such as root distribution and surface ponding depth [*Zhu and Mohanty*, 2003, 2004, 2006;

[1]Department of Biological and Agricultural Engineering, Texas A&M University, College Station, Texas, USA.
[2]Now at International Research Institute for Climate and Society, The Earth Institute, Columbia University, Palisades, New York, USA.

Corresponding author: B. P. Mohanty, Department of Biological and Agricultural Engineering, Texas A&M University, 2117 TAMU, 201 Scoates Hall, College Station, TX 77843, USA. (bmohanty@tamu.edu)

0043-1397/12/2010WR009581

Zhu et al., 2004, 2006]. The soil hydraulic properties were also influenced by vertical heterogeneity (e.g., tillage practice, pore size distribution due to structural cracks and root development and decay, textural layering and geology), and parameter estimations could vary in the vertical direction [*Mohanty et al.*, 1994; *Mallants et al.*, 1996]. Although *Mohanty and Zhu* [2007] investigated effective soil hydraulic parameter averaging schemes for steady state flow in heterogeneous shallow subsurface useful to land-atmosphere interaction modeling, not many studies have been carried out to explore issues for vertical subsurface heterogeneity associated with various soil types.

[6] In this study, we adopted a layer-specific soil moisture assimilation scheme for determining the soil hydraulic parameters in layered soil profiles. The main objective is to analyze the impact of soil layering associated with various soil textural combinations in the profile and to quantify the one-dimensional soil hydraulic properties of different soil layers in the root zone (0–200 cm) based on the layer-specific soil moisture assimilation scheme. This work could be useful to characterize hydrologic systems that are instrumented to measure root zone soil moisture. Additionally, this approach may serve as a basis for developing futuristic analytical platforms to characterize vadose zone systems at regional and global scales by synthesizing profile soil moisture data collected using various ground-, air-, and space-based sensors of different spectral frequencies and penetrating depths.

2. Materials and Methods

2.1. One-Dimensional Layer-Specific Soil Moisture

2.1.1. Conceptual Framework

[7] The aim of the layer-specific soil moisture assimilation scheme is to estimate the soil moisture retention $\theta(h)$ and hydraulic conductivity $K(h)$ curves in a layered soil column (e.g., 1st, 0–10 cm; 2nd, 10–60 cm; and 3rd, 60–200 cm) by optimizing the effective soil hydraulic parameters for each layer based on a simulation-optimization [*Ines and Droogers*, 2002]. As depicted in Figure 1, the approach uses the soil moisture in the layers (here, we set up at 5 cm depth for the 1st and 2nd layers and at 10 cm depth for the 3rd layer) to estimate the layer specific soil hydraulic properties. The choice on locations of soil moisture measurements in the soil profile to be used in the simulation-optimization can be established in a more systematic way. Mathematically, the soil hydraulic parameters are obtained by finding a set of soil hydraulic parameter $\mathbf{p}$ such that the differences between observed $\theta_i(t)$ and simulated $\theta_i\ (t;\ p_i)$ soil moisture at soil layers i, are minimized; where $\mathbf{p} = p_{i=1,\ldots,M}$; and p_i is the corresponding soil hydraulic parameters in the individual soil layers. The choice of objective function is critical in inverse modeling; from sensitivity analysis (see section 3.3) we selected the additive absolute form (equation (1)) as it produced better results than other forms considered in this study (e.g., multiplicative and additive squared delta); $Z(\mathbf{p})$ is the objective function, M is the number of soil layers, N is the time domain, and t is the index for time.

$$Z(\mathbf{p}) = \min\left\{\frac{1}{N}\frac{1}{M}\sum_{t=1}^{N}\sum_{i=1}^{M}|\theta_i(t) - \theta_i(t;p_i)|\right\}. \quad (1)$$

2.1.2. Description of the SWAP Model

[8] SWAP is a physically based model that simulates the processes of the soil–water–atmosphere–plant system [*van Dam et al.*, 1997]. The soil moisture dynamics $\theta_i(t)$ in the soil column can be described using the one-dimensional Richards' equation (equation (2)). SWAP model solves

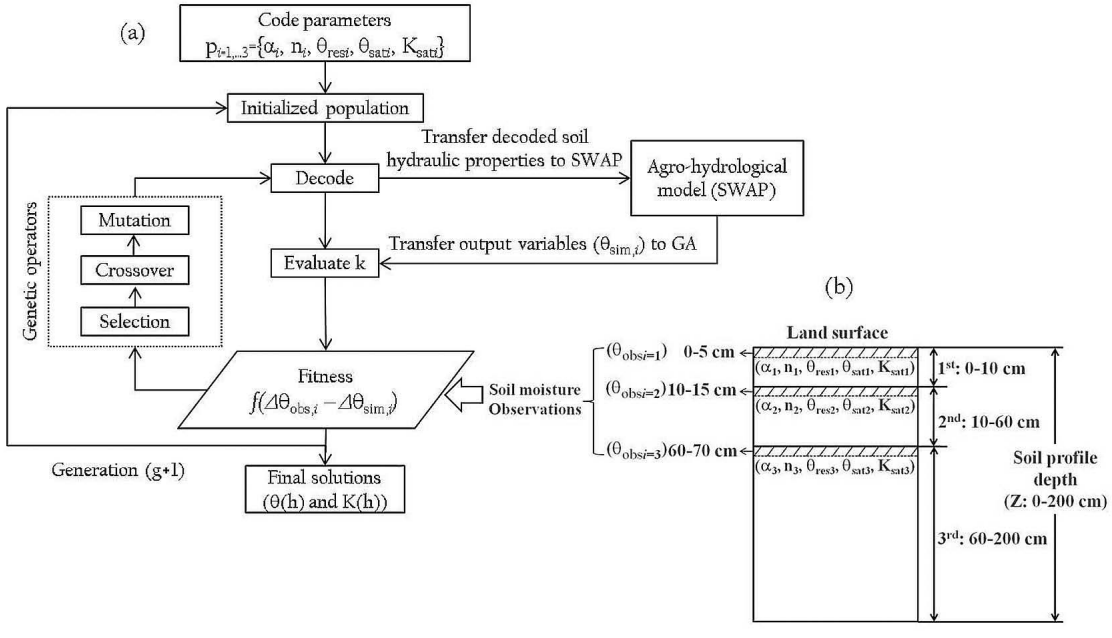

Figure 1. (a) Schematic diagram of layer-specific soil moisture assimilation scheme (SWAP-GA linkage) based on inverse modeling, and (b) layered soil column.

equation (2) numerically using the implicit finite difference scheme [*Belmans et al.* 1983],

$$\frac{\partial\theta(z,t)}{\partial t} = C(h(z,t))\frac{\partial h(z,t)}{\partial t} = \frac{\partial\left[K(h(z,t))\left(\frac{\partial h(z,t)}{\partial z}+1\right)\right]}{\partial z} - S(h,z,t), \quad (2)$$

where K is the hydraulic conductivity (cm d^{-1}), h is the soil water pressure head (−cm), z is the vertical soil depth (cm) taken positively upward, C is the differential water capacity (cm^{-1}), and $S(h, z, t)$ is the actual soil moisture extraction rate by plant roots (cm^3 cm^{-3} d^{-1}) defined as equation (3).

$$S(h,z,t) = \begin{cases} \alpha_w(h,z,t)\dfrac{T_{pot}(t)}{Z_r}; & z < Z_r \\ 0; & z > Z_r \end{cases}, \quad (3)$$

where T_{pot} is the potential plant transpiration (cm d^{-1}), Z_r is the rooting depth (cm), and α_w is a reduction factor as function of h (at depth z and time t) and accounts for water deficit and oxygen stress [*Feddes et al.*, 1978].

[9] The soil hydraulic functions are described by analytical expressions of *van Genuchten* [1980] and *Mualem* [1976].

$$S_e(h,z,t) = \frac{\theta(h(z,t)) - \theta_{res}}{\theta_{sat} - \theta_{res}} = \left[\frac{1}{1+|\alpha h(z,t)|^n}\right]^m, \quad (4)$$

$$K(h,z,t) = K_{sat}S_e(h,z,t)^{\lambda}[1-(1-S_e(h,z,t)^{1/m})^m]^2, \quad (5)$$

where S_e is the relative saturation (−), θ_{res} and θ_{sat} are the residual and saturated water contents (cm^3 cm^{-3}), α (cm^{-1}), n (−), m (−), and λ (−) are shape parameters of the retention and the conductivity functions, K_{sat} is the saturated hydraulic conductivity (cm d^{-1}), and $m = 1 - 1/n$.

[10] The SWAP model considers for several combinations of the top (atmospheric) and bottom boundary conditions [*van Dam et al.*, 1997]. Moreover, it contains water management modules for irrigation and drainage modules as well as process-based crop growth models including WOFOST for simulating the impacts of weather, soil type, plant type, and water management on the crop growth [*van Dam et al.*, 1997, *van Dam*, 2000]. The SWAP model calculates the potential evapotranspiration (ET_{pot}) according to the Penman-Monteith equation using daily meteorological data. The partition of ET_{pot} rate into potential transpiration rate (T_{pot}) and potential evaporation rate (E_{pot}) is determined by the leaf area index or the soil cover fraction. The potential evapotranspiration (ET_{pot}) is calculated using the minimum value of canopy resistance and actual resistance. Then the actual evapotranspiration (ET_{act}) is calculated by the root water uptake reduction due to water and salinity stress.

2.1.3. Genetic Algorithm

[11] Genetic algorithms (GAs) are powerful search algorithms based on the precept of natural selection [*Holland*, 1975; *Goldberg*, 1989]. The unknown parameters in a search problem are represented by genes, which are arranged in an array called chromosome. The search starts by initializing a population of chromosomes becoming the starting points in the search across the search surface. The suitability of a chromosome is evaluated using a fitness function. Based on their fitness, they are selected to the mating pool, reproduce through the process of crossover, and allowed to mutate. The solution of the search problem would be the fittest chromosome that survives after many generations. In this study, a modified-*micro*GA was used to search for the parameter set (**p**) by minimizing the error between the simulated and observed soil moisture in the layered soil column. The modified-*micro*GA is a GA variant that uses a micro population to search for the solution of the inverse problem. The uniqueness in the modified-*micro*GA is the ability to restart when the chromosomes of the micropopulation are nearly 90% similar in structure, allowing more micropopulation restarts [*Ines and Droogers*, 2002; *Caroll*, 1996; *Goldberg*, 2002; *Krishnakumar*, 1989; D. L. Carroll, Fortran genetic algorithm (GA) driver, available at www.cuaerospace.com/carroll/ga.html]. The modified-*micro*GA allows a creep mutation (at base 10). *Ines and Mohanty* [2008a] added an intermittent jump mutation to further introduce new genetic materials during the search. A time saving mechanism was designed by remembering not only the elite chromosome of the previous generation (g-1) but also its remaining chromosomes such that when they are generated in the next generation, there is no need to run them anymore in the SWAP model, saving computational time [*Ines and Honda*, 2005]. The elite chromosome is always reproduced in the next generation.

[12] The modified-*micro*GA was applied to the inverse modeling (IM)-based layer-specific soil moisture assimilation scheme [*Ines and Droogers*, 2002; *Ines and Mohanty*, 2008a, 2008b]. The search spaces for each Mualem-Van Genuchten parameters in the multilayered soil system as used in this study are shown in Table 1.

2.1.4. Parameter Uncertainty

[13] When an elitist modified-*micro*GA converges to the solution, all of the chromosomes in a population are almost similar. To create some sort of uncertainty bounds to the solution, a multipopulation generated by various random number generator seeds (e.g., −1000, −950, and −750) were run concurrently. After many generations, the average fitness of all the chromosomes from the multipopulations is calculated and classified as above or below average. The above average solutions are considered as the most probable solutions. The 95 percent confidence interval (95PCI) of the most probable solutions was calculated as,

$$\mathrm{Range}_{p,s,t,i} = 95\mathrm{pci}_{p,s,t,i+} \quad 95\mathrm{pci}_{p,s,t,i-}, \quad (6)$$

where $95PCI_{p,s,t,i+}$ and $95PCI_{p,s,t,i-}$ are the upper and lower boundary of the 95PCI, p is the soil hydraulic parameter, s is the index of soil type, t is the time (running) index, and i is the soil layers.

[14] Pearson's correlation (R^2) and uncertainty analysis (Mean Absolute Error-MAE, Mean Bias Error-MBE, and Root Mean Square Error-RMSE) between observed and

Table 1. Summary of the Parameter Constraints in the Genetic Algorithm[a]

Parameter	Search Space		No. of Bit (L)	Binary (2^L)
	Min. Values	Max. Values		
		Cases 1 and 2		
α	0.006	0.033	5	2^5 (32)
n	1.200	1.610	6	2^6 (64)
θ_{res}	0.061	0.163	7	2^7 (128)
θ_{sat}	0.370	0.550	5	2^5 (32)
K_{sat}	1.840	55.700	10	2^{10} (1024)
		Case 3 (LW 02 and 11)		
α	0.006	0.033	5	2^5 (32)
n	1.200	2.200	6	2^6 (64)
θ_{res}	0.040	0.163	7	2^7 (128)
θ_{sat}	0.340	0.550	5	2^5 (32)
K_{sat}	1.840	250.000	10	2^{10} (1024)
		Case 3 (LW 07)		
α	0.006	0.033	5	2^5 (32)
n	1.200	2.200	6	2^6 (64)
θ_{res}	0.040	0.163	7	2^7 (128)
θ_{sat}	0.340	0.550	5	2^5 (32)
K_{sat}	1.840	130.000	10	2^{10} (1024)

[a]Total search space = 32 × 64 × 128 × 32 × 1024 = 8,589,934,592. Example of $\mathbf{p} = \{\alpha, n, \theta_{res}, \theta_{sat}, K_{sat}\}$ = {00101, 110010, 0001111, 00001, 0101000101}. Probability of crossover = 0.5. Probability of creep mutation = 0.5. Probability of intermittent jump mutation = 0.05. Population = 10 chromosomes. Number of multipopulation = 3. Maximum generation = 500.

simulated data are also used to assess the performance of the modified-*micro*GA,

$$R_i^2 = \frac{\sum_{t=1}^{n}(\hat{\theta}_{sim,i,t} - \overline{\theta}_{sim,i})(\theta_{obs,i,t} - \overline{\theta}_{obs,i})}{\sqrt{\sum_{t=1}^{n}(\hat{\theta}_{sim,i,t} - \overline{\theta}_{sim,i})^2 \sum_{t=1}^{n}(\theta_{obs,i,t} - \overline{\theta}_{obs,i})^2}}, \quad (7)$$

$$\left.\begin{aligned} \mathrm{MAE}_i &= \frac{1}{n}\sum_{t=1}^{n}|(\theta_{obs,i,t} - \hat{\theta}_{sim,i,t})| \\ \mathrm{MBE}_i &= \frac{1}{n}\sum_{t=1}^{n}(\theta_{obs,i,t} - \hat{\theta}_{sim,i,t}) \\ \mathrm{RMSE}_i &= \sqrt{\frac{1}{n}\sum_{t=1}^{n}(\theta_{obs,i,t} - \hat{\theta}_{sim,i,t})^2} \end{aligned}\right\}, \quad (8)$$

where, $\hat{\theta}_{sim,i,t}$ is the average soil moisture of different populations with the time index (t), $\overline{\theta}_{sim,i}$ is the average of $\hat{\theta}_{sim,i,t}$, $\theta_{obs,i,t}$ is the observed soil moisture for the time index (t), and $\overline{\theta}_{obs,i}$ is the average of $\theta_{obs,i,t}$, respectively. Note that the MBE and RMSE were tested only for the field experiments.

2.2. Numerical Experiments

[15] This study estimates the effective soil hydraulic parameters in a layered soil column adopting the layer-specific soil moisture assimilation scheme based on the inverse modeling approach [*Ines and Mohanty*, 2008a, 2008b, 2009]. The numerical experiments were conducted for three cases: (1) case 1: layered soil column with free drainage, (2) case 2: layered soil column with varying water table depths (i.e., −200, −150, and −100 cm from the soil surface), and (3) case 3: field experiments.

[16] The soil profile layering is given as follows: the 1st (top 0–10 cm), 2nd (10–60 cm), and 3rd (60–200 cm) soil layers (Figure 2). The topsoil moisture (1st, 0–5 cm; 2nd, 10–15 cm; 3rd, 60–70) below the soil interfaces were only extracted and used for quantifying the soil hydraulic parameters in the soil layers for Cases 1 to 3, respectively. In real-world conditions, soil profiles are irregularly layered, thus the decision for selecting the layer depths where soil moisture observations will be compared with simulations should be based upon the available data. For all the simulations, the soil column was discretized into 33 computational layers. The first soil layer was finely discretized at intervals of 1 cm. The second and third soil layers were discretized at intervals of 5 and 10 cm (except 33rd layer with 20 cm discretization), respectively. For the free-draining case, the initial soil water pressure head distribution in the soil profile was prescribed uniformly at −150 cm. For the cases with groundwater table bottom boundaries, they are prescribed with initial soil water pressure head distribution in hydrostatic equilibrium with the initial water table depths. Various land covers (bare soil, grass, and wheat) representative of annual crops in the study area (Little Washita Watershed, Oklahoma) were considered for the numerical experiments.

[17] In the hypothetical cases, we used the soil hydraulic parameter values from the UNSODA database as reference soil hydraulic data for the given soils in each soil layers. Using the weather data at the Little Washita (ARS 134) site in 1997, we generated synthetic daily soil moisture datasets using SWAP in a forward mode. These daily soil moisture data were then used to estimate back the soil hydraulic parameters for the layered system. Several field sites were selected to evaluate the applicability of the layer-specific soil moisture assimilation scheme under actual field condition in case 3 (Figure 3). Some details of the different cases are given below.

2.2.1. Case 1: Layered Soil Column Under Free Drainage Condition

[18] Some of the uncertainties in the estimation of soil hydraulic parameters in the soil system can be associated with various environmental factors (e.g., root density, rooting depth, soil layers, different combinations of soil types, and profile arrangement, etc.). For this reason, we conducted nine inverse modeling scenarios for case 1 comprising of various soil types, soil layers, and vegetation combinations. As base case scenarios, the six scenarios were composed of layer combinations of sandy loam, silt loam, and clay loam along the soil profile with grass cover. These scenarios aimed at assessing the effects of soil layering and heterogeneity in the subsurface (Table 2, where CB1 to 6 denote soil layering combinations).

[19] The other three scenarios included varying the vegetation covers, e.g., bare soil, grass, and wheat to evaluate the impact of varying vegetations in the layer specific data assimilation procedure using only the CB 5 case (Table 2). Also analyzed are the interactions between water stress by crops (T_{act}/T_{pot}) and near-surface (0–5 cm) soil moisture changes near the land surface using the CB 5. This study considered only rain-fed conditions for the numerical cases.

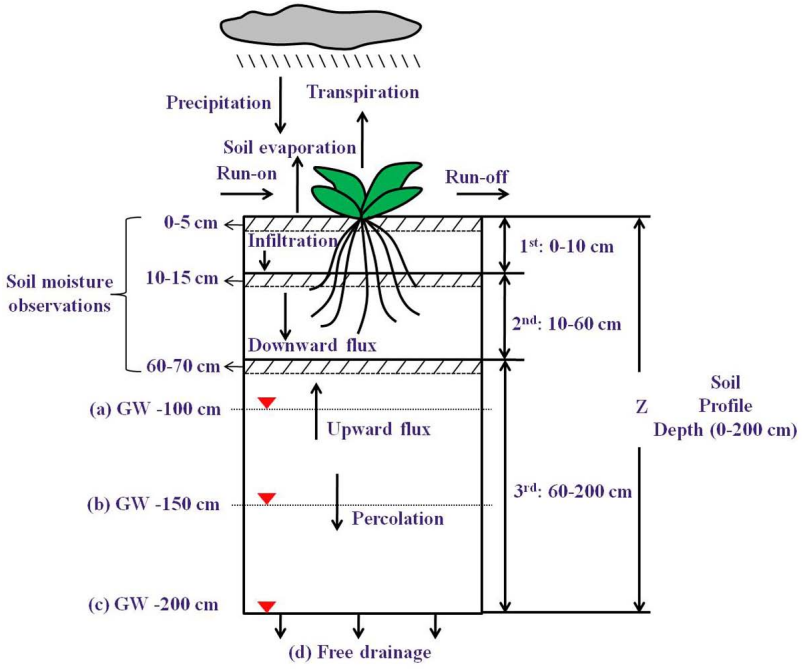

Figure 2. Layered soil column used in the numerical experiments with free drainage and various groundwater (GW) table depths; (a) GW −100 cm, (b) GW −150 cm, (c) GW −200 cm, and (d) free drainage.

2.2.2. Case 2: Layered Soil Column Under Various Groundwater Table Conditions

[20] Under cases when soil moisture dynamics in the unsaturated zone is governed significantly by shallow water table, additional experiments with various water table depths (−200, −150, and −100 cm from the soil surface) were conducted. This case aimed to assess the effects of groundwater on the estimates of effective soil hydraulic properties (only for CB 5 in case 1—grass cover) using the layer-specific soil moisture assimilation approach.

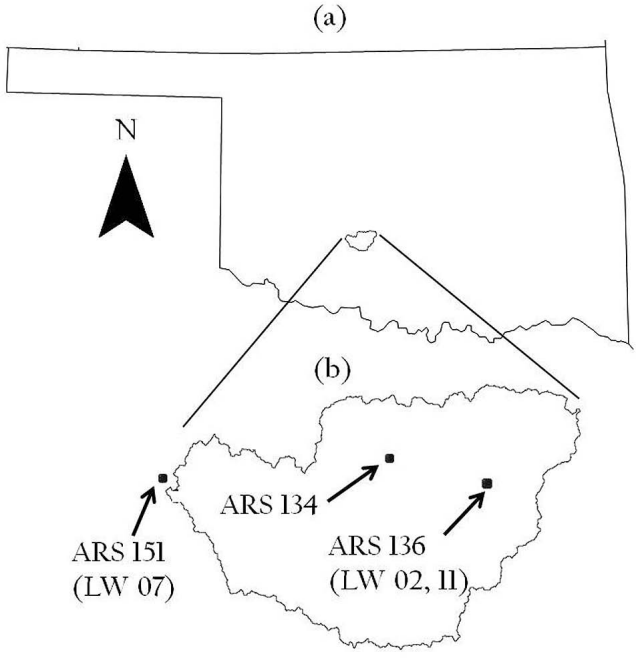

Figure 3. The study area; (a) Oklahoma, (b) the Little Washita (LW 02, 07, and 11) watershed.

2.2.3. Case 3: Field Experiments

[21] The layer-specific soil moisture assimilation scheme was applied to the several field monitoring sites within the Little Washita (LW 02, 07, and 11) watershed in Oklahoma using datasets from the Southern Great Plains Hydrology Experiment 1997 (SGP97) [*Mohanty et al.*, 2002; *Heathman et al.*, 2003, *Das and Mohanty*, *2006*].

[22] Daily weather datasets (e.g., precipitation, solar radiation, relative humidity, minimum and maximum temperature, and wind speed) were collected at the USDA Agricultural Research Service (ARS 136 and 151) micronet and the Oklahoma Mesonet weather stations from January 1–December 31, 1997. The LW 02, 07, and 11 sites are characterized by a mixture of loam, sandy loam, and sandy loam with grass covers, with a rooting depth of (up to) 100–120 cm [*Mohanty et al.*, 2002; Table 3]. The bottom boundary condition was unknown at the field sites. Therefore, we tested free-drainage conditions and several groundwater table depths (−100, −150, and −200 cm) as bottom boundaries and selected the bottom boundary condition (free-drainage conditions for the LW 02, 07, and 11 were selected), with the best performance (fitness) obtained by the genetic algorithm.

[23] In this study, the soil core samples extracted from the different soil depths (1st, 0–5 cm; 2nd, 30–35 cm; 3rd, 60–65 cm for LW 02; and 1st, 0–5 cm; 2nd, 20–25 cm; 3rd, 40–45 cm for LW 07) collected during the SGP97 (18 June to 18 July, 1997) were analyzed to obtain the soil hydraulic parameters in the laboratory experiment. Using

Table 2. Combinations of Three Soil Types for Case 1

Depth	Combinations (CB) of Three Soil Types					
	CB 1	CB 2	CB 3	CB 4	CB 5	CB 6
First (0–10 cm)	Sandy loam	Sandy loam	Silt loam	Silt loam	Clay loam	Clay loam
Second (10–60 cm)	Silt loam	Clay loam	Sandy loam	Clay loam	Sandy loam	Silt loam
Third (60–200 cm)	Clay loam	Silt loam	Clay loam	Sandy loam	Silt loam	Sandy loam

the laboratory derived soil hydraulic properties, we estimated the soil moisture in the soil layers for the field sites with the hydrological (SWAP) model in a forward modeling mode. These soil moisture data were used to estimate back the heterogeneous soil hydraulic properties across the soil profile to test if the layer specific assimilation method could successfully match the laboratory derived soil hydraulic parameters (also known as, forward-backward modeling under actual field condition setting). This part of the study does not serve as a validation of the method because there were no measured soil moisture profile data available at the sites to derive independently the layer soil hydraulic parameters, but aimed to ascertain the utility of the approach under field conditions. We compared the derived soil hydraulic properties by inverse modeling, with UNSODA soil hydraulic data [*Leij et al.*, 1999] and the laboratory-derived data.

[24] The case of LW 11 is more of calibration-validation study. The daily (*in-situ*) soil moisture observations (21 days; DOY: 169–181) measured by the time domain reflectometer (TDR) probe in the soil layers (1st, 0–5 cm; 2nd, 20–25 cm; 3rd, 40–45 cm) were used for calibration, then validation runs were done for DOY: 182–197. Validation here means that we used the derived layered soil hydraulic parameters to simulate soil moisture for the remaining days. The modeling soil column was composed of three layers (1st, 0–20 cm; 2nd, 20–40 cm; 3rd, 40–60 cm for LW 11) determined by the depths at where the soil moisture were measured. The derived soil hydraulic parameters were compared with laboratory-derived parameters (no data at deeper depths from our SGP97 hydraulic property database near-by).

3. Results and Discussions

[25] In this study, various combinations of soil layers, soil types, vegetations, and groundwater table depths are used for studying their impacts on estimation of soil hydraulic parameters in a layered soil domain. The following sections present the results of the inverse modeling experiments.

3.1. Case 1: Layered Soil Column Under Free Drainage Condition

[26] We estimated the $\theta(h)$ and $K(h)$ curves in the layered soil profile using the combinations (CB 1 to 6) of three soil types in Figure 4. The estimated $\theta(h)$ in CB 1 to 6 corresponded well with the reference curves although the uncertainty bounds showed increasing trends with soil depths. On the other hand, the estimated $K(h)$ in the layered soil profile is more uncertain than $\theta(h)$, suggesting that $K(h)$ is more difficult to estimate than $\theta(h)$ in a layered system with soil moisture information only being used in the inverse modeling. We observed that soil hydraulic parameter estimation is influenced not only by soil layering, but also the order/sequence of vertical heterogeneity in the soil profile. CB 6 for example, although clay loam and silt loam soils were located in the 1st and 2nd layers, their $\theta(h)$ and $K(h)$ uncertainty bounds have broader range (more uncertainty) than those at the 3rd layer, while when they are located in other arrangements, they are better identified.

[27] Table 4 presents the correlations (R^2) and uncertainties (MAE) of observed and simulated soil moisture dynamics in the top portion (near the soil layer interfaces) of the 1st (between 0–5 cm), 2nd (between 10–15 cm), and 3rd (between 60–70 cm) soil layers for the 6 combinations involving three different soil types at the ARS 134 site. Mostly, the simulated soil moisture estimates in the soil layers matched well with the observations in the range of R^2 (1st, 0.974–0.999; 2nd, 0.978–0.998; 3rd, 0.980–0.997) and MAE (1st, 0.004–0.016; 2nd, 0.004–0.020; 3rd, 0.001–0.012) as shown in Figure 4.

[28] Figure 5 shows the daily precipitation, water stress (T_{act}/T_{pot}), and soil moisture changes for CB 5 (only shown here for CB5 case). Under the rain-fed condition, the water

Table 3. Field-Scale Soil Texture and Soil Hydraulic Properties in the Layered Soil Column at the LW 02, 07, and 11 Sites

Number of Soil Layers	Depth Increment[a]	Sand[a] (%)	Silt[a] (%)	Clay[a] (%)	Soil Texture[a]	α[a]	n[a]	θ_{res}[a]	θ_{sat}[a]	K_{sat}[a]	Vegetation Rooting Depth (cm)
					LW 02						
First layer	0–30 cm	40.47	43.15	16.37	Loam (L)	0.012	1.679	0.127	0.397	114.650	Up to 120
Second layer	30–60 cm	40.47	41.38	18.14	Loam (L)	0.013	1.505	0.091	0.397	203.560	Up to 120
Third layer	60–90 cm	35.66	45.59	18.75	Loam (L)	0.027	1.616	0.102	0.482	238.120	Up to 120
					LW 07						
First layer	0–20 cm	83.89	8.61	7.50	Loam sand (LS)	0.011	2.112	0.061	0.348	53.533	Up to 100
Second layer	20–40 cm	65.86	20.39	13.75	Sandy loam (SL)	0.016	1.736	0.048	0.345	65.837	Up to 100
Third layer	40–60 cm	61.82	24.43	13.75	Sandy loam (SL)	0.021	1.711	0.091	0.387	120.100	Up to 100
					LW 11						
First layer	0–20 cm	59.13	21.40	19.47	Sandy loam (SL)	0.019	1.460	0.046	0.416	186.190	Up to 100

[a]Field observations [*Mohanty et al.*, 2002].

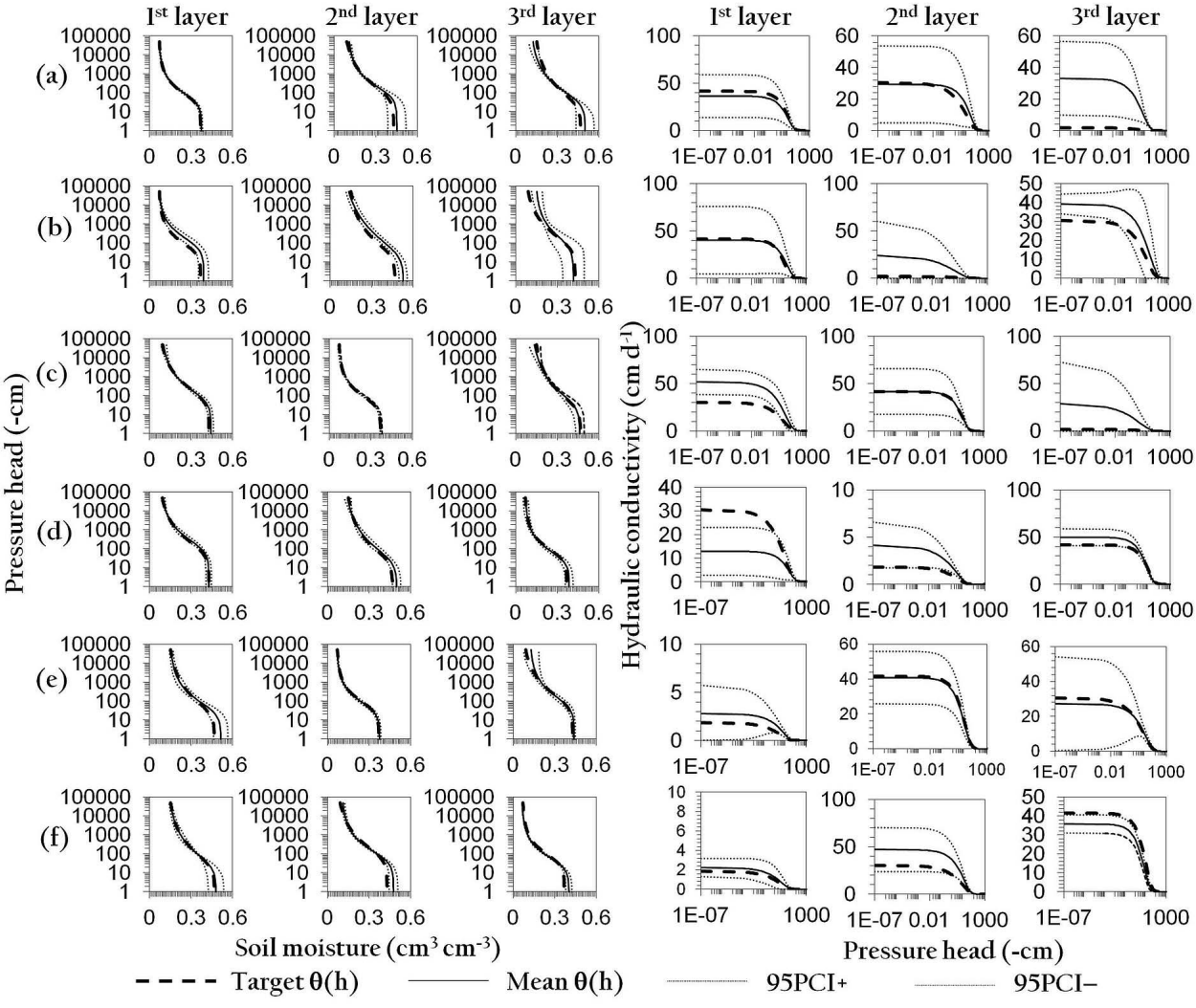

Figure 4. Derived $\theta(h)$ and $K(h)$ functions of the layered soil column with grass for case 1 using the layer-specific soil moisture assimilation scheme; (a) CB1: 1st-sandy loam, 2nd-silt loam, 3rd-clay loam, (b) CB2: 1st-sandy loam, 2nd-clay loam, 3rd-silt loam, (c) CB3: 1st-silt loam, 2nd-sandy loam, 3rd-clay loam, (d) CB4: 1st-silt loam, 2nd-clay loam, 3rd-sandy loam, (e) CB5: 1st-clay loam, 2nd-sandy loam, 3rd-silt loam, (f) CB6: 1st-clay loam, 2nd-silt loam, 3rd-sandy loam.

stress by the crop (grass) corresponded to the weather condition. As the near-surface soil moisture becomes dry, the water stress level for the CB 5 increased considerably during the dry periods indicating that the plant activities were affected by the dry condition near the land surface. The soil moisture estimates in all the layers were identified well with the target values and the uncertainties in the 1st layer (between 0–5 cm depth) are higher than those in the 2nd (between 10–15 cm depth) and 3rd (between 60–70 cm depth) layers. It is evident that there are uncertainties involved in $\theta(h)$ and $K(h)$ estimates, because the soil moisture estimates reflect uncertainties associated with various

Table 4. Correlations (R^2) and Mean Absolute Error (MAE) of Soil Moisture Dynamics at 0–5 cm, 10–15 cm, and 60–70 cm Depths in the Layered Soil Column Using the $\theta(h)$ and $K(h)$ Functions Derived by the Layer-Specific Soil Moisture Assimilation Scheme at the ARS 134 Site for Case 1[a]

	CB1		CB2		CB3		CB4		CB5		CB6	
Depth	R^2	MAE	R^2	MAE	R^2	MAE	R^2	MAE	R^2	MAE	R^2	MAE
First (0–5 cm)	0.989	0.007	0.974	0.016	0.998	0.006	0.999	0.004	0.996	0.013	0.998	0.013
Second (10–15 cm)	0.992	0.007	0.978	0.020	0.998	0.004	0.998	0.004	0.990	0.004	0.995	0.006
Third (60–70 cm)	0.980	0.006	0.997	0.012	0.990	0.009	0.997	0.001	0.996	0.001	0.994	0.005

[a]Correlations are indicated with R^2. For Case 1, CB 1 to 6: free drainage with grass.

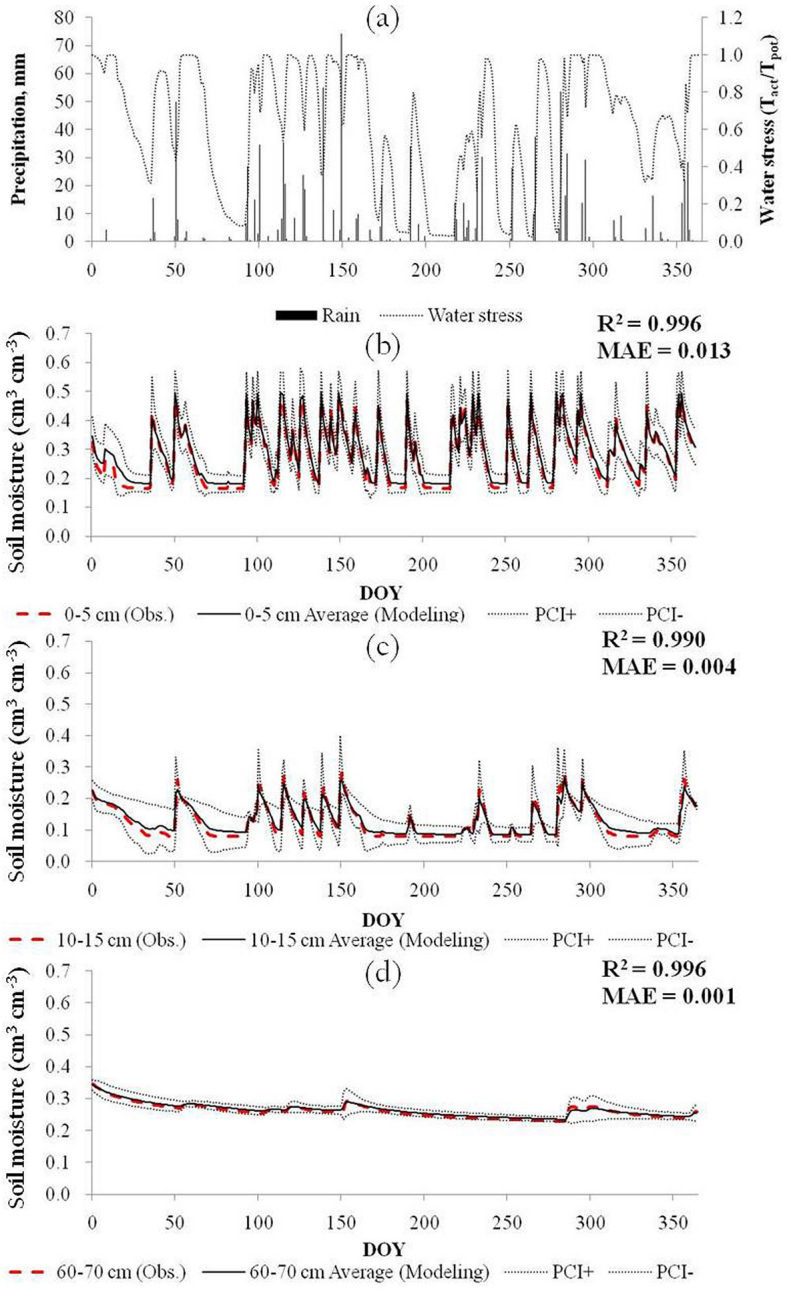

Figure 5. (a) Daily precipitation (mm) and water stress (T_{act}/T_{pot}) and (b–d) root zone soil moisture dynamics (cm^3 cm^{-3}) at 0–5 cm, 10–15 cm, and 60–70 cm depths in the layered soil column using the $\theta(h)$ and $K(h)$ functions derived by the layer-specific soil moisture assimilation scheme at the ARS 134 site (case l-CB 5: free drainage with grass).

conditions (e.g., vegetation covers, soil hydraulic properties or meteorological data, as well as functional errors of the hydrological model itself for estimating the soil moisture). The correlation (R^2) and MAE values of the simulated and observed (hypothetical) soil moisture estimates in the numerical experiments range from 0.990 to 0.996 and 0.001 to 0.013, respectively.

[29] Various land covers (e.g., bare soil, grass, and wheat) were applied to CB 5 as shown in Table 5. The soil hydraulic parameters with the bare soil cover were better identified with the target values than those with grass and wheat, although the estimates in the 2nd and 3rd layers have uncertainties, especially for K_{sat}. In the cases of grass and wheat, the parameter uncertainties in the 1st and 3rd layers were considerably higher than those in the 2nd layer. This is more evident when compared with the results of bare soil, which indicates that complexities incurred by plant root activities to soil moisture dynamics in the root zone. The parameters in the 3rd layer have more uncertainties than those in the 1st and 2nd layers with all vegetation covers as shown in Table 5. There are no apparent differences between grass and wheat vegetations, although the K_{sat}

Table 5. Solutions of the Layer-Specific Soil Moisture Assimilation Scheme of CB 5 With Bare Soil, Grass, and Wheat Vegetations for Case 1—Layered Soil Column[a]

		Bare Soil		Grass		Wheat	
Parameter	Target Values[b]	Mean	PCI	Mean	PCI	Mean	PCI
			First Soil Layer				
α	0.030	0.031	0.028–0.033	0.028	0.020–0.036	0.031	0.029–0.032
n	1.370	1.393	1.292–1.493	1.492	1.269–1.715	1.423	1.332–1.514
θ_{res}	0.129	0.132	0.088–0.177	0.141	0.106–0.176	0.141	0.114–0.169
θ_{sat}	0.470	0.474	0.457–0.490	0.515	0.463–0.566	0.480	0.465–0.495
K_{sat}	1.840	2.397	0.765–4.029	2.817	–0.140–5.775	2.004	1.808–2.200
			Second Soil Layer				
α	0.021	0.027	0.018–0.035	0.023	0.019–0.028	0.022	0.021–0.024
N	1.610	1.577	1.562–1.592	1.605	1.596–1.614	1.597	1.577–1.617
θ_{res}	0.067	0.062	0.060–0.064	0.065	0.061–0.068	0.065	0.061–0.069
θ_{sat}	0.370	0.376	0.371–0.381	0.375	0.365–0.384	0.373	0.364–0.381
K_{sat}	41.600	52.466	43.918–61.015	39.984	23.391–56.578	31.019	17.579–44.459
			Third Soil Layer				
α	0.012	0.010	0.005–0.014	0.014	0.005–0.024	0.014	0.010–0.017
N	1.390	1.384	1.218–1.550	1.530	1.368–1.692	1.446	1.320–1.572
θ_{res}	0.061	0.063	0.059–0.066	0.117	0.050–0.184	0.119	0.021–0.217
θ_{sat}	0.430	0.404	0.380–0.429	0.441	0.432–0.450	0.429	0.421–0.437
K_{sat}	30.500	16.446	8.964–23.927	27.237	0.280–54.193	26.960	24.898–29.021

[a]Wheat vegetations 1st, clay loam; 2nd, sandy loam; 3rd, silt loam.
[b]UNSODA database [*Leij et al.*, 1999].

values in the 2nd and 3rd layers with grass are better identified than those with wheat.

3.2. Case 2: Layered Soil Column Under Varying Groundwater Table Conditions

[30] This analysis is done only for the CB 5 soil-layering scenario. Table 6 shows the summary of results of the layered soil column with the groundwater table depths of −200, −150, and −100 cm from the soil surface. We can see a visible trend which indicates that the soil hydraulic parameters in the 1st, 2nd, and 3rd layers with the presence of deeper groundwater (GW) table depth of −200 cm are identified better than the estimates for the scenarios with shallow GW tables at −150 and −100 cm. The α, n, and θ_{res} values for GW −200 cm in the 1st layer correspond well with the target values, while only the α values for GW −150 and −100 cm have a good matching with the target values. For the 2nd layer, the solutions of the hydraulic parameters (α, n, θ_{res}, and θ_{sat}) for all the groundwater table depths of −200, −150, and −100 cm are better matched compared to the results of the 1st layer indicating that it may be affected by the root activities more than other

Table 6. Solutions of the Layer-Specific Soil Moisture Assimilation Scheme of CB 5 for Case 2—Layered Soil Column With Ground Water Tables[a]

		GW −200 cm		GW −150 cm		GW −100 cm	
Parameter	Target Values[b]	Mean	PCI	Mean	PCI	Mean	PCI
			First				
α	0.030	0.032	0.029–0.034	0.031	0.027–0.034	0.032	0.030–0.033
n	1.370	1.372	1.235–1.508	1.389	1.237–1.542	1.459	1.189–1.728
θ_{res}	0.129	0.127	0.098–0.156	0.136	0.089–0.184	0.136	0.076–0.196
θ_{sat}	0.470	0.502	0.444–0.560	0.481	0.465–0.497	0.498	0.415–0.582
K_{sat}	1.840	5.815	−1.383–13.013	2.390	1.448–3.333	3.637	0.107–7.166
			Second				
α	0.021	0.020	0.019–0.021	0.020	0.016–0.023	0.022	0.016–0.029
N	1.610	1.587	1.563–1.611	1.600	1.577–1.622	1.600	1.588–1.612
θ_{res}	0.067	0.063	0.057–0.070	0.065	0.058–0.072	0.097	0.042–0.152
θ_{sat}	0.370	0.375	0.365–0.385	0.374	0.362–0.385	0.371	0.367–0.375
K_{sat}	41.600	30.290	24.131–36.449	27.303	25.044–29.562	34.917	−1.796–71.629
			Third				
α	0.012	0.013	0.006–0.019	0.009	0.003–0.016	0.008	0.003–0.013
N	1.390	1.497	1.366–1.628	1.434	1.109–1.760	1.515	1.419–1.610
θ_{res}	0.061	0.141	0.104–0.178	0.122	0.069–0.175	0.125	0.052–0.198
θ_{sat}	0.430	0.423	0.356–0.490	0.411	0.361–0.462	0.422	0.405–0.440
K_{sat}	30.500	31.778	14.576–48.980	20.487	10.982–29.992	51.981	37.939–66.023

[a]The scheme for CB5 is 1st, clay loam; 2nd, sandy loam; 3rd, silt loam. The ground water tables are at −200, −150, and −100 cm.
[b]UNSODA database [*Leij et al.*, 1999].

layers as shown in Table 5. Overall, the parameter estimations at the GW −200 cm are matched better with the target values than those at the GW −150 and −100 cm. Especially, as the groundwater table is lowered, the n, θ_{sat}, and K_{sat} values at the GW −150 cm in the 1st layer were identified better than those for the GW −100 cm indicating that the parameter estimations at the upper layers are influenced by the upward flows from shallow groundwater table [see *Ines and Mohanty*, 2008a].

[31] In the 3rd layer, close to groundwater boundary, only α and K_{sat} values are identifiable with the target values. The errors of estimation in the 3rd layer are considerably worse than those in the 1st and 2nd layers. The inverse solutions for case 2 (in the presence of groundwater tables) have more uncertainties than for case 1 (well drained). In general, the uncertainty range (±95PCI) of soil hydraulic parameters with GW at −200 cm is smaller than those for GW at −150 and −100 cm. It confirms that soil hydraulic estimates in the layered soil column are governed not only by soil layering but also by the bottom boundary conditions, especially in the presence of shallow groundwater table.

3.3. Case 3: Field Validation Experiment

[32] Figures 6 and 7 show the daily rainfall and simulated/observed soil moisture in the 1st (LW 02, 0–30 cm; and LW 07, 0–20 cm), 2nd (LW 02, 30–60 cm; and LW 07, 20–40 cm), and 3rd (LW 02, 60–90 cm; and LW 07, 40–60 cm) layers at the field sites during the simulation period based on the inverse modeling. In general, $\theta(h)$ at the LW 02 and 07 sites derived by the layer-specific soil moisture assimilation scheme matched well with the observations, although uncertainties exist in the estimated $\theta(h)$ functions for the 1st, 2nd, and 3rd layers. When we compared the K_{sat} values of UNSODA database and laboratory-based experiments in Table 1 and 3, the laboratory-based K_{sat} values were extremely higher than those of UNSODA database due to measurement errors. Thus, we excluded the $K(h)$ functions for further analysis due to its nonsensitivity. The simulated soil moisture (1st, $R^2 = 0.998$ and MAE = 0.011; 2nd, $R^2 = 0.997$ and MAE = 0.001; 3rd, $R^2 = 0.992$ and MAE = 0.002 for LW 02; and 1st, $R^2 = 0.991$ and MAE = 0.005; 2nd, $R^2 = 0.992$ and MAE = 0.003; 3rd, $R^2 = 0.993$ and MAE = 0.003 for LW 07) estimates in the layered soil column identified well with the estimates derived by the soil hydraulic parameters taken near the LW 02 and 07 sites. The soil moisture estimates in the 1st layer at the field sites have more uncertainties than those in 2nd and 3rd layers. These results are in agreement with the results of CB5 in case 1, which indicate that the estimated soil moisture with the grass cover in the 2nd and 3rd layers are closer to the target values than those in the 1st layer, as shown in Figure 5. The derived soil hydraulic properties compared well with UNSODA, based on dominant textural class. Figure 8 shows the measured (TDR-based) and simulated soil moisture dynamics in the soil layers at the LW 11 site. Overall, the simulated results (R^2: 0.891, MAE: 0.018 for the 1st layer; R^2: 0.967, MAE: 0.006 for the 2nd layer; R^2: 0.894, MAE: 0.034 for the 3rd layer) for the calibration period matched well with the measurements. The result (R^2: 0.965, MAE: 0.051 for the 1st layer; R^2: 0.891, MAE: 0.035 for the 2nd layer; R^2: 0.949, MAE: 0.037 for the 3rd layer) for the validation period also shows the good matching in the soil layers at the field site. The derived soil hydraulic parameters by inverse modeling in the 1st layer (0–20 cm) compared well with the independently measured soil hydraulic parameters from laboratory. Table 7 presents the uncertainty analysis of estimated soil moisture dynamics for the soil layers using various objective functions (additive absolute value, multiplicative absolute value, and additive square delta forms) with three different methods (MAE, MBE, and RMSE) at the LW 11 site. It is clear that the additive absolute value form of the objective function used in this study produced better results than by the multiplicative and square delta forms for the calibration and validation. Also, The MAE and RMSE performed similarly during the calibration and validation whereas the MBE was less sensitive than others.

[33] Although this method has a limitation (available measurements in the soil layers), it gives us insights of the implication/impact of soil heterogeneity and layering in quantifying soil hydraulic parameters in the layered soil column. With more in situ soil moisture networks in place globally (e.g., Oklahoma Mesonet, Soil Climate Analysis Network: SCAN, USDA-Agricultural Research Service: USDA-ARS network, National Ecological Observatory Network: NEON, International Soil Moisture Network: ISMN, etc.) and data available in the recent years at multiple soil depths from benchmark experiments, this layer-specific assimilation method can prove to be quite useful for predicting the soil moisture dynamics in the soil layers.

4. Conclusion

[34] In this study, a layer-specific soil moisture assimilation procedure based on simulation-optimization (SWAP-GA) scheme was developed to quantify effective soil hydraulic parameters in the layered soil profile. Various numerical experiments with the conditions of free drainage, presence of groundwater tables at several different depths, different vegetation covers, and field experiments were conducted. The impacts of soil layers, heterogeneity of different soil textures, and different land covers in a vertically layered soil column were evaluated in case 1 using the layer-specific soil moisture assimilation scheme. Case 2 was conducted to evaluate the impacts of various groundwater table depths with a grass cover. The field experiments of case 3 were conducted for assessing the applicability of this approach at the field-scales (LW 02, 07, and 11 sites).

[35] The results of case 1 show that the soil layers and order/sequence of vertical heterogeneity of soil textures affect the uncertainties of parameter estimations due to complex signature of soil water in the layered soil profile. Also, the estimated parameters in the 1st and 3rd layers with the grass and wheat covers have relatively more errors than that of the bare soil. It may indicate that the hydrological model has the own weakness for simulating plant root activities in the root zone. In case 2, we found that as the groundwater table becomes deeper, the estimates of soil hydraulic parameters improved as well as the results with the free drainage condition. These results suggest that the bottom boundary condition has a large influence on the hypothesis of layer-specific data assimilation studies. In the field experiments of case 3, the soil moisture dynamics and

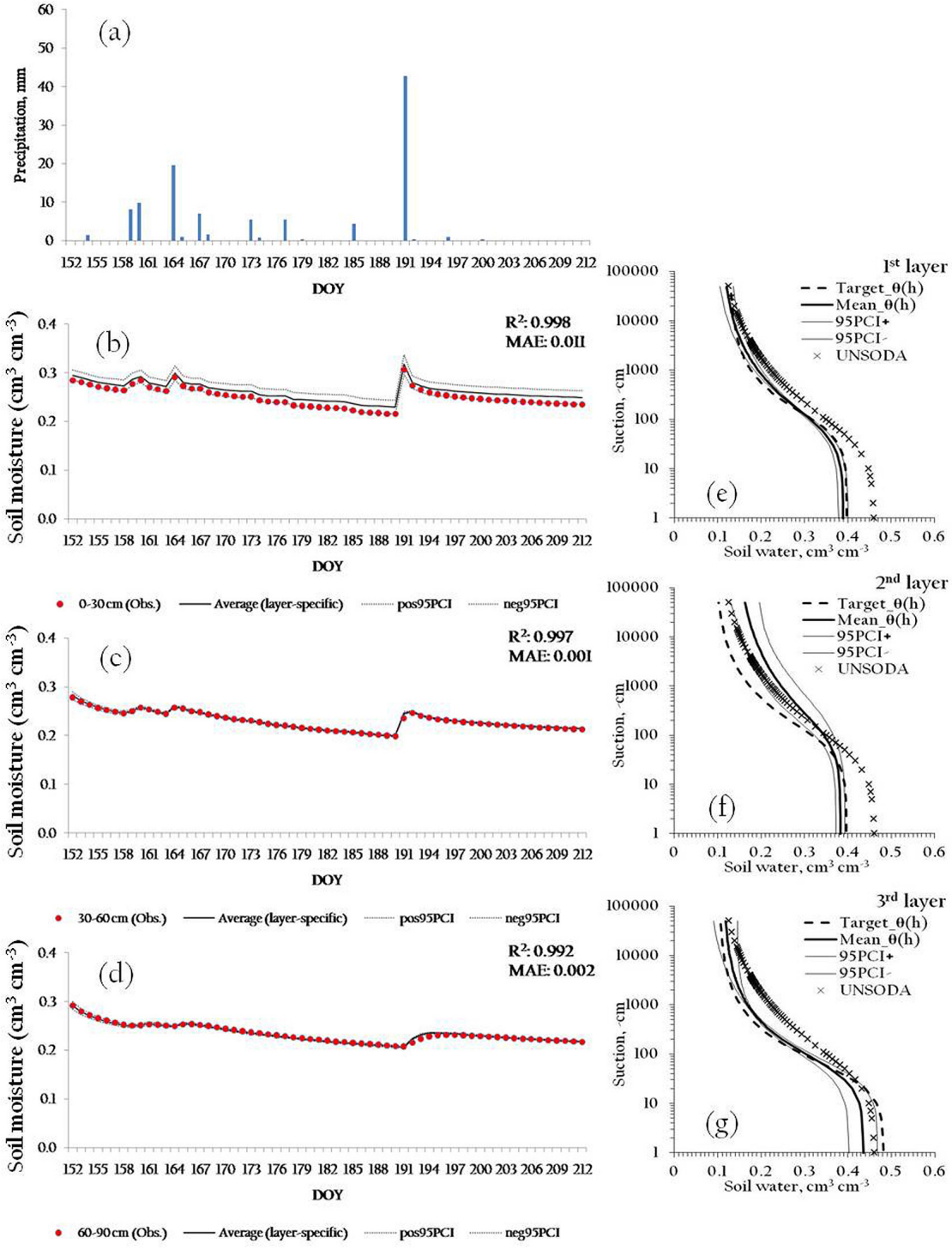

Figure 6. (a) Daily precipitation (mm), (b–d) observed/simulated root zone soil moisture dynamics, and (e–g) $\theta(h)$ functions of target, derived solutions, and UNSODA database (dominated by loam soil) at the 1st (0–30 cm), 2nd (30–60 cm), and 3rd (60–90 cm) in the LW 02 site (ARS 136) using the layer-specific soil moisture assimilation scheme.

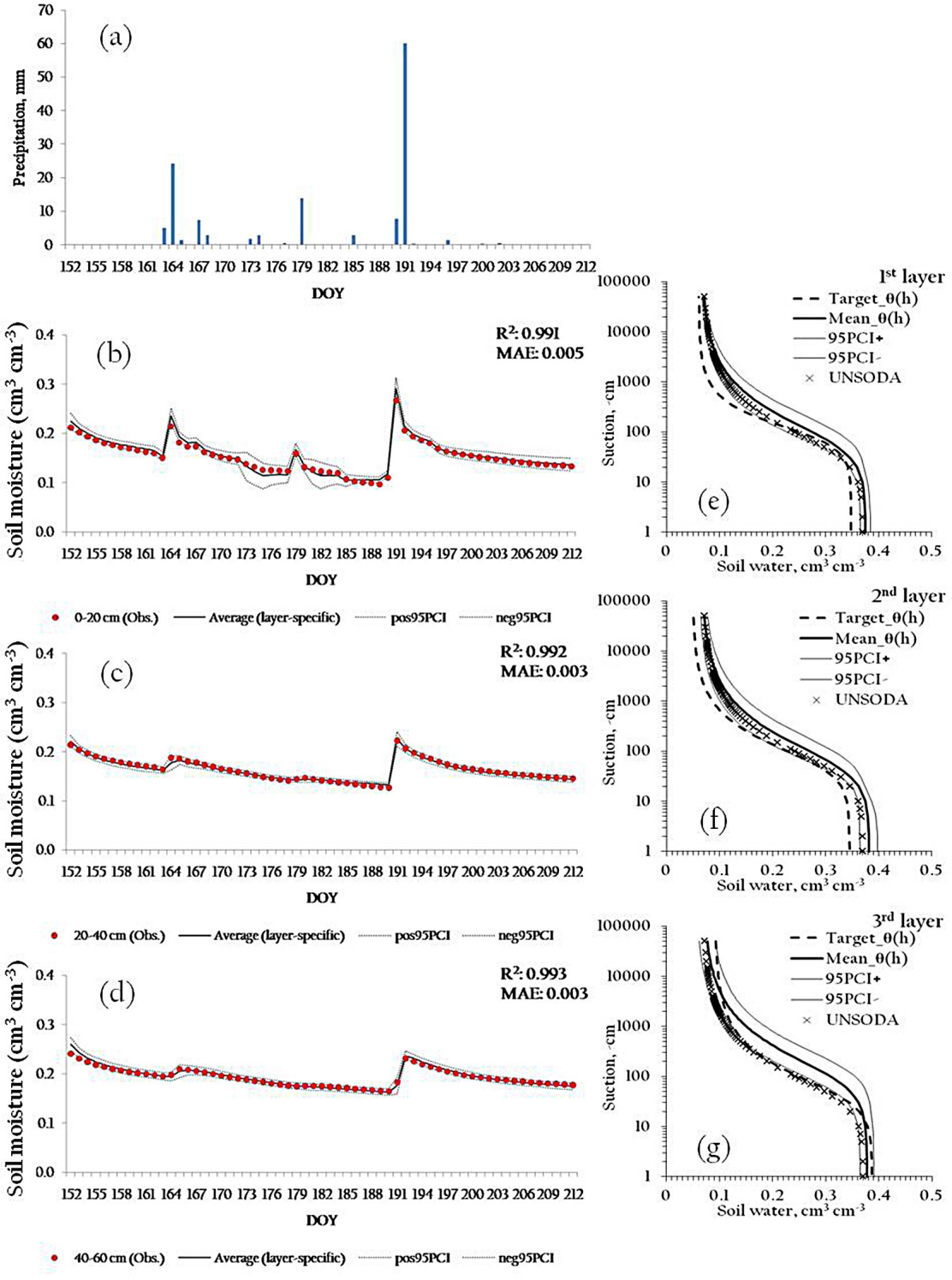

Figure 7. (a) Daily precipitation (mm), (b–d) observed/simulated root zone soil moisture dynamics, and (e–g) $\theta(h)$ functions of target, derived solutions, and UNSODA database (dominated by sandy loam soil) at the 1st (0–30 cm), 2nd (30–60 cm), and 3rd (60–90 cm) in the LW 07 site (ARS 151) using the layer-specific soil moisture assimilation scheme.

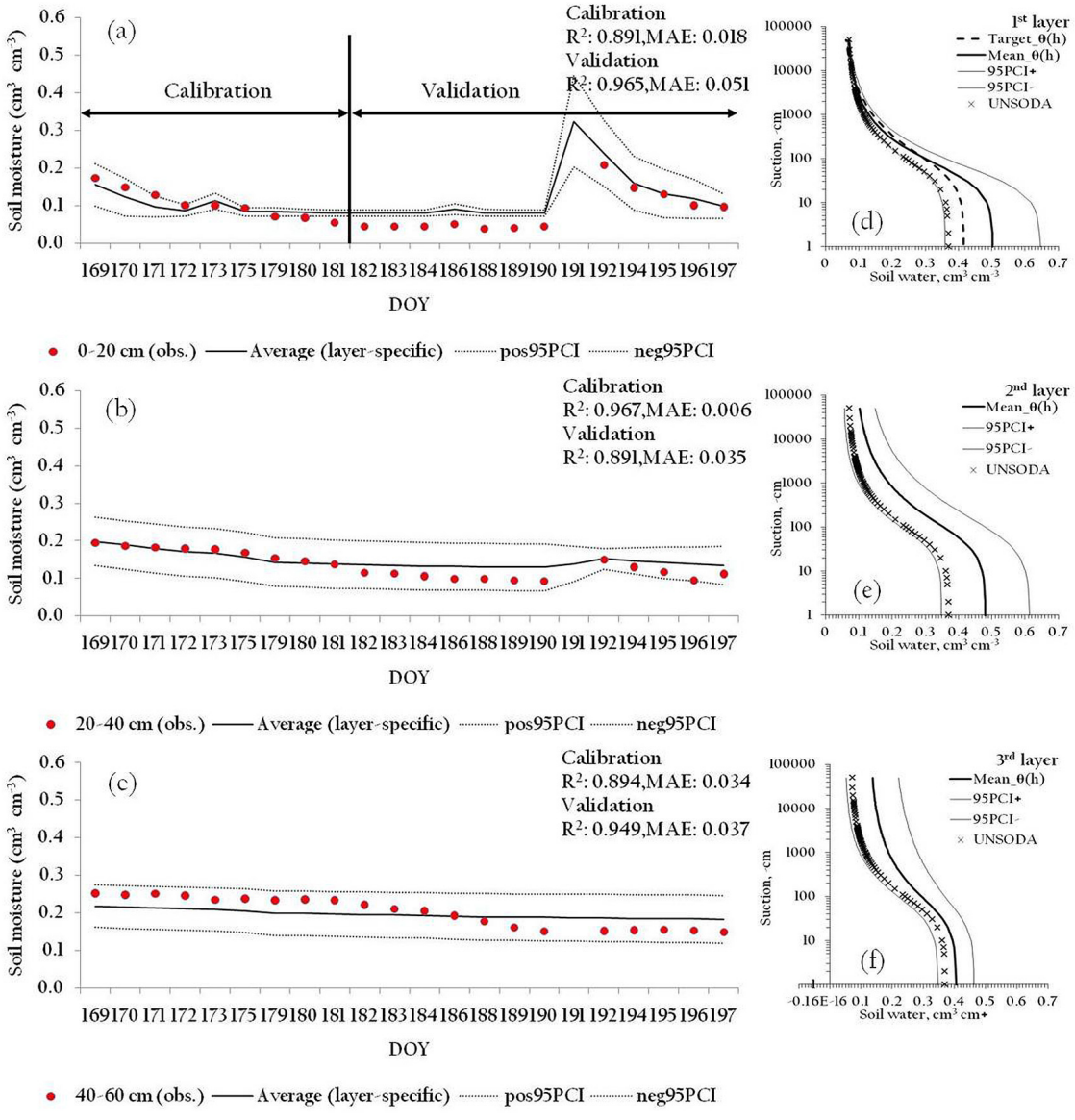

Figure 8. (a–c) Observed (*in-situ*) and simulated root zone soil moisture dynamics and (d–f) $\theta(h)$ functions of target (1st layer was only measured), derived solutions, and UNSODA database (dominated by sandy loam soil) at the 1st (0–20 cm), 2nd (20–40 cm), and 3rd (40–60 cm) in the LW 11 site (ARS 136) using the layer-specific soil moisture assimilation scheme during the calibration (DOY 169-181) and validation (DOY 182-197) periods.

$\theta(h)$ functions were only estimated at the LW 02 and 07 sites using the layer-specific soil moisture assimilation scheme, because of the limited observations. The simulated near-surface and subsurface soil moisture estimates at the field sites identified well with the field observations (derived by the soil hydraulic parameters obtained from the soil core samples collected at the field sites), even though the soil moisture estimates near the land surface have slightly higher uncertainties than those in the deeper soil layers. The simulated soil moisture dynamics in the soil layers were also matched well with the in situ measurements for the LW 11 site. It suggests that the layer-specific assimilation scheme based on inverse modeling could be used to model soil moisture dynamics in the layered soil profile even with the limited soil moisture measurements in the real world conditions. We envisaged that the new soil moisture assimilation procedure would be useful for vadose zone and land surface modeling in well-instrumented hydrologic system. In future, with the advent of advanced soil moisture remote sensing capabilities with deeper penetrating depths, this layer-specific assimilation platform can be useful for estimating large-scale effective soil hydraulic properties under heterogeneous/layered soil condition, as the near-surface assimilation proved to be useful in homogeneous soil conditions in the past studies [*Ines and Mohanty*, 2008a, 2008b, 2009].

Table 7. Uncertainty Analysis Using Various Objective Functions With Three Different Methods Based on the Layer-Specific Soil Moisture Assimilation Scheme During the Calibration and Validation Periods[a]

	Additive Absolute Form				Multiplicative Form				Additive Square Delta Form			
Soil Layers	R^2	MAE	MBE	RMSE	R^2	MAE	MBE	RMSE	R^2	MAE	MBE	RMSE
					Calibration							
First[b]	0.891	0.018	0.004	0.006	0.972	0.017	−0.017	0.007	0.979	0.027	−0.027	0.010
Second[c]	0.967	0.006	0.004	0.002	0.971	0.058	−0.058	0.019	0.963	0.013	0.008	0.005
Third[d]	0.894	0.034	0.034	0.011	0.886	0.067	−0.067	0.022	0.891	0.021	0.021	0.007
					Validation							
First[b]	0.965	0.051	−0.051	0.026	0.994	0.073	−0.073	0.032	0.996	0.079	−0.079	0.034
Second[c]	0.891	0.035	−0.035	0.013	0.023	0.094	−0.094	0.028	0.009	0.047	−0.046	0.016
Third[d]	0.949	0.037	−0.029	0.016	0.940	0.133	−0.133	0.040	0.943	0.044	−0.041	0.018

[a]The objective functions are additive absolute, multiplicative, and additive square delta forms. The three different methods are Mean Absolute Error-MAE, Mean Bias Error-MBE, and Root Mean Square Error-RMSE. The layer-specific soil moisture assimilation scheme that the calculations are based on is, during the calibration, DOY 169-181, and during the validation, DOY 182-197.
[b]The layer at 0–20 cm.
[c]The layer at 20–40 cm.
[d]The layer at 40–60 cm.

[36] **Acknowledgments.** The research was funded by NASA-THP grant (NNX08AF55G, NNX09AK73G) and NSF (CMG/DMS) grants (0621113, C10-00021).

References

Belmans, C., J. G. Wesseling, and R. A. Feddes (1983), Simulation of the water balance of a cropped soil, SWATRE, *J. Hydrol.*, *63*, 271–286.

Bosch, D. D. (1991), Error associated with point observation of matric potential in heterogeneous soil profiles, *Trans. ASAE*, *34*(6), 2427–2436.

Brooks, R. H., and A. T. Corey (1964), Hydraulic properties of porous media, *Hydrol. Pap. 3*, 27 pp., Colo. State Univ., Fort Collins, Colo.

Carroll, D. L. (1996), Genetic Algorithms and optimizing chemical oxygen-Iodine lasers, in *Developments in Theoretical and Applied Mechanics*, Vol. 18, edited by H. B. Wilson et al., pp. 411–424, Sch. of Eng., Univ. of Ala., Tuscaloosa.

Das, N. N., and B. P. Mohanty (2006), Root zone soil moisture assessment using passive microwave remote sensing and vadose zone modeling, *Vadose Zone J.*, *5*, 296–307.

Feddes, R. A., P. J. Kowalik, and H. Zarandy (1978), Simulation of field water use and crop yield, *Simul. Monogr.*, Pudoc. Wageningen, Netherlands.

Gardner, W. R. (1958), Some steady state solutions of unsaturated moisture flow equations with application from a water table, *Soil Sci.*, *85*, 228–232.

Goldberg, D. E. (1989), *Genetic algorithms in search and optimization and machine learning*, Addison-Wesley Publ., Reading, MA.

Goldberg, D. E. (2002), *The Design of Innovation: Lessons From and for Competent Genetic Algorithms*, Kluwer Acad., Norwell, Mass.

Green, R. E., L. R. Ahuja, and S. K. Chong (1986), Hydraulic conductivity, diffusivity, and sorptivity of unsaturated soils: Field methods, in *Methods of Soil Analysis, Part 1. Physical and Mineralogical Methods*, edited by A. Klute, *Monogr. Am. Soc. Agron., 9*, 771–798.

Hansen, J. D., Rojas, K. W. and M. J. Schaffer (1999), Calibrating the root zone water quality model, *Agron. J.*, *91*, 171–177.

Heathman, G. C., P. J. Starks, L. R. Ahuja, and T. J. Jackson (2003), Assimilation of surface soil moisture to estimate soil water content, *J. Hydrol.*, *279*: 1–17, doi:10.1016/S0022-1694(03)00088-X.

Holland, J. H. (1975), On quantifying agricultural and water management practices from low spatial resolution RS data using genetic algorithms: a numerical study for mixed pixel environment, *Adv. Water Resour.*, *28*, 856–870.

Ines, A. V. M., and P. Droogers (2002), Inverse modeling in estimating soil hydraulic functions: A genetic algorithm approach, *Hydrol. Earth Syst. Sci.*, *6*(1), 49–65.

Ines, A. V. M., and K. Honda (2005), On quantifying agricultural and water management practices from low spatial resolution RS data using genetic algorithms: A numerical study for mixed pixel environment, *Adv. Water Resour.*, *28*, 856–870.

Ines, A. V. M., and B. P. Mohanty (2008a), Near-surface soil moisture assimilation for quantifying effective soil hydraulic properties using genetic algorithm: 1. Conceptual modeling, *Water Resour. Res.*, *44*, W06422, doi:10.1029/2007WR005990.

Ines, A. V. M., and B. P. Mohanty (2008b), Near-surface soil moisture assimilation for quantifying effective soil hydraulic properties under different hydro-climatic conditions, *Vadose Zone J.*, *7*, 39–52.

Ines, A. V. M., and B. P. Mohanty (2009), Near-surface soil moisture assimilation for quantifying effective soil hydraulic properties using genetic algorithm: 2. With airborne remote sensing during SGP97 and SMEX02, *Water Resour. Res.*, *45*, W01408, doi:10.1029/2008WR007022.

Jana, R. B., and B. P. Mohanty (2012a), A topography-based scaling algorithm for soil hydraulic parameters at hillslope scales: Field testing, *Water Resour. Res.*, *48*, W02519, doi:10.1029/2011WR011205.

Jana, R. B., and B. P. Mohanty (2012b), A comparative study of multiple approaches to soil hydraulic parameter scaling applied at the hillslope scale, *Water Resour. Res.*, *48*, W02520, doi:10.1029/2010WR010185.

Krishnakumar, K. (1989), Microgenetic algorithms for stationary and non-stationary function optimization, in *Proc. SPIE: Intelligent Control and Adaptive System*, vol. 1196, edited by G. Rodriguez, pp. 289–296, SPIE, Philadelphia, Pa.

Leij, F. J., W. J. Alves, M. T. Van Genuchten, and J. R. Williams (1999), The UNSODA unsaturated soil hydraulic database, in *Characterization and Measurement of the Hydraulic Properties of Unsaturated Porous Media*, edited by M. T. Van Genuchten, F. J. Leij, and L. Wu, pp. 1269–1281, Univ. of Calif., Riverside, Calif.

Mallants, D., B. P. Mohanty, D. Jacques, and J. Feyen (1996), Spatial variability of hydraulic properties in a multi-layered soil, *Soil Sci.*, *161*(3), 167–181.

Mohanty, B. P., and J. Zhu (2007), Effective soil hydraulic parameters in horizontally and vertically heterogeneous soils for steady-state land-atmosphere interaction, *J. Hydrometeorol.*, *8*, 715–729.

Mohanty, B. P., R. S. Kanwar and C. J. Everts (1994), Comparison of saturated hydraulic conductivity measurement methods for a glacial till soil, *Soil Sci. Soc. Am. J.*, *58*(3), 672–677.

Mohanty, B. P., P. J. Shouse, D. A. Miller, and M. T. van Genuchten (2002), Soil property database: Southern Great Plains 1997 Hydrology Experiment, *Water Resour. Res.*, *38*(5), 1047, doi:10.1029/2000WR000076.

Mualem, Y. (1976), A new model for predicting the hydraulic conductivity of unsaturated porous media, *Water Resour. Res.*, *12*, 513–522.

Nielsen, D. R., J. W. Biggar, and K. T. Her (1973), Spatial variability of field measured soil-water properties, *Hilgardia*, *42*, 215–259.

Rose, C. W., W. R. Stern, and J. E. Drummond (1965), Determination of hydraulic conductivity as a function of depth and water content for soil in situ, *Aust. J. Soil Res.*, *3*, 1–9.

Stockton, J. G., and A. W. Warrick (1971), Spatial variability of unsaturated hydraulic conductivity, *Soil Sci. Soc. Am. J.*, *35*, 847–848.

van Bavel, C. H. M., G. B. Stirk, and K. J. Brust (1968), Hydraulic properties of a clay loam soil and the field measurement of water uptake by roots: I. Interpretation of water content and pressure profiles, *Soil Sci. Soc. Am. Proc.*, *32*, 310–317.

van Dam, J. C. (2000), Field-scale water flow and solute transport. SWAP model concepts, parameter estimation and case studies, Ph.D. thesis, Wageningen Univ., Wageningen, Netherlands.

van Dam, J. C., J. Huygen, J. G. Wesseling, R. A. Feddes, P. Kabat, P. E. V. van Waslum, P. Groenendjik, and C. A. van Diepen (1997), Theory of SWAP version 2.0: Simulation of water flow and plant growth in the soilwater-atmosphere-plant environment, *Tech. Doc. 45*, DLO Winand Staring Cent., Wageningen Agric. Univ., Wageningen, Netherlands.

van Genuchten, M. T. (1980), A closed-form equation foe predicting the hydraulic conductivity of unsaturated soils, *Soil Sci. Soc. Am. J.*, *44*, 892–898.

Vrugt, J. A., G. Schoups, J. W. Hopmans, C. Young, W. W. Wallender, and W. Bouten (2004), Inverse modeling of large-scale spatially distributed vadose zone properties using global optimization, *Water Resour. Res.*, *40*, W06503, doi:10.1029/2003WR002706.

Wood, E. F. (1994), Scaling, soil moisture and evapotranspiration in runoff models, *Adv. Water Resour.*, *17*, 24–34.

Zhu, J., and B. P. Mohanty (2002), Upscaling of hydraulic properties for steady state evaporation and infiltration, *Water Resour. Res.*, *38*(9), 1178, doi:10.1029/2001WR000704.

Zhu, J., and B. P. Mohanty (2003), Upscaling of hydraulic properties in heterogeneous soils, in *Scaling Methods in Soil Physics*, edited by Y. Pachepsky, D. E. Radcliffe, and H. M. Selim, pp. 97–117, CRC Press, Boca Raton, Fla.

Zhu, J., and B. P. Mohanty (2004), Soil hydraulic parameter upscaling for steady-state flow with root water uptake, *Vadose Zone J.*, *3*, 1464–1470.

Zhu, J., and B. P. Mohanty (2006), Effective scaling factors for transient infiltration in heterogeneous soils, *J. Hydrol.*, *319*, 96–108.

Zhu, J., B. P. Mohanty, A. W. Warrick, and M. T. van Genuchten (2004), Correspondence and upscaling of hydraulic functions for steady-state flow in heterogeneous soils, *Vadose Zone J.*, *3*, 527–533.

Zhu, J., B. P. Mohanty, and N. N. Das (2006), On the effective averaging schemes of hydraulic properties at the landscape scale, *Vadose zone J.*, *5*, 308–316.